UNIVERSITÀ DEGLI STUDI DI TORINO

Efficient green protocols for the preparation of highly functionalized β-cyclodextrin grafted silica

Katia Martina[†], Francesca Baricco[†], Gloria Berlier[‡], Marina Caporaso[†] and Giancarlo Cravotto*,[†]

[†] Department of Drug Science and Technology and NIS - Nanostructured Interfaces and Surfaces Centre of Excellence, University of Turin, Via P. Giuria 9, 10125 Turin (Italy).

[‡] Department of Chemistry and NIS - Nanostructured Interfaces and Surfaces Centre of Excellence, University of Turin, Via P. Giuria 7, 10125 Turin, Italy.

* Author to whom correspondence should be addressed:

giancarlo.cravotto@unito.it; Fax: +39 011 6707687

ABSTRACT

The modification and characterization of porous particles and matrices using cyclodextrins (CD) has attracted a large amount of interest in recent years. In fact, CDs are at the heart of this study which aims to graft β-CD onto silica particles by means of efficient protocols and non-conventional energy sources. In particular, the use of microwave irradiation, benign reaction media and a solvent-free planetary ball mill has provided a high degree of grafting. The inclusive properties of β-CD grafted silica were tested with phenolphthalein and its sorption capacity with

methyl orange and both tests confirmed the efficiency of the grafting protocols. Samples were extensively characterized by TGA, elemental analysis, IR, BET and HRTEM. The green protocols herein reported can facilitate access to functionalized silica and pave the way to its use in novel applications.

Keywords: Silica, Cyclodextrin, Microwaves, Mechanochemistry, Green Chemistry

Introduction

In recent times, silica has become an ubiquitous inorganic platform that is used in material science including catalysis, separation, filtration, sensing, optoelectronics and environmental technology.[1-3] This is primarily because of the advantageous properties that silica displays, such as excellent stability (chemical and thermal), mechanical robustness, good accessibility and porosity. Secondly, the silica surface includes a number of silanol groups which can be grafted with organic molecules. Functionalized silica surfaces display very different properties to the native material.[4-6]

The classic technique for grafting and modifying the silica surface involves the use of condensation reactions between silanol groups and alkoxy- or chloro-silanes.[7] The development of synthetic procedures that enable high organic substance loading efficiencies has become an important goal because of an increase in interest in the biological applications of surface technologies,[8-10] such as enzyme immobilization, DNA, peptide, protein and carbohydrate microarrays. The immobilization of highly functionalized molecules onto solid-support surfaces via Click chemistry affords a facile approach to useful composite materials.[11, 12, 13]

Green Chemistry uses a set of principles that aims to reduce or eliminate the use or generation of hazardous substances in the design, manufacture and application of chemical products.[14,15]

One of its key areas is the replacement of hazardous solvents in chemical processes with benign media such as water.[16,17] The development of solvent-free alternative processes is, of course, the best solution.[18] The concept of replacing conventional processes with enabling techniques, such as microwaves (MW) or solvent-free mechanochemical activation using ball mills, has truly blossomed in the literature.[19] Although MW-assisted reactions in organic solvents have developed rapidly,[20,21] focus has now shifted to environmentally friendly methods which use greener solvents.[22]

Silica immobilized CDs have been extensively studied for use as stationary phases in chiral chromatography via HPLC and GC.[23,24,25] Most heterogeneous catalysts are based on silica supports and often undergo surface modification to confer higher activity.[26-29] The functional groups of such hybrid organic-inorganic materials may serve as anchoring sites for metal complexes and several publications have made reference to the preparation of a silica-CD-metal catalyst.[30] CDs have been also employed for the preparation of nanodevices that self-assemble on surfaces of mesoporous silica nanoparticles and which are used to regulate the controlled release of cargo/drug molecules via a range of external stimuli. The CDs in this application are covalently bound to the silica,[31] while rotaxanes/pseudorotaxanes on surfaces have often been studied. All these studies have achieved useful functionality and have provided stimuli-induced macroscopic effects on the basis of switchable host-guest systems.[32-34] Our experience in the field has helped us notice that, besides significant interest in CD grafted silica, there is a lack of work on the preparation of highly covalently functionalized systems in the literature. Furthermore, only a few publications reported s detailed characterization and quantification of the CD grafted on silica.[35,36]

In this account, we report our recent investigation into a very efficient green synthesis of highly functionalized silica grafted CDs. We have used MW irradiation in benign reaction media such as water and solventless protocols in a planetary ball. The study includes an extensive characterization of the prepared samples which quantifies synthetic efficiency and underlines the physical properties of the CD-grafted silica samples obtained under these non-conventional methods.

Experimental session

Materials and Equipment.

All commercially available reagents and solvents were used without further purification. Sipernat 320 amorphous silica was supplied by Evonik Degussa. Reactions were carried out in professional MW reactors: a monomode system (Monowave 300®, Anton-Paar GmbH) and a multimode rotating reactor (Rotosynth®, Milestone srl). Mechanochemistry was performed in a Planetary Ball Mill PM100 (Retsch GmbH).

Preparation of 3-Glycidyloxypropyl silica (Si- GPMS)

(3-Glycidoxypropyl)methyldiethoxysilane (0.934 mL, 0.420 mol) was dissolved in the solvent (10 mL) and silica SIPERMAT 320 (1 g) was added. The suspension was either heated under stirring in an oil bath (80 °C for 5 h) or in a MW reactor (80 °C for 1 h, average power 26 W using water as solvent, or 53 W in toluene). The modified silica was then filtered, washed thoroughly and dried under vacuum.

When performed under mechanochemical activation, the milling beakers (50 mL, stainless steel) were charged with two types of milling balls; 48 stainless steel balls at a diameter of 5 mm and 1500 stainless steel balls at a diameter 2 mm. 300 µL of (3-glycidoxypropyl)

methyldiethoxysilane and 1 g of silica were added. Milling was carried out at 200 rpm for 20 min. After cooling to room temperature, the modified silica was tested as described above.

Preparation of Si-G-Und

Si- GPMS (1 g) and 10-undecynil-1-amine (0.275 g, 1.64 mmol) were dissolved in DMF (3 mL). The solution was heated to 80 °C and stirred for 24 h. The silica was finally filtered and washed with DMF, water and toluene and dried under vacuum. The same procedure was repeated under MW irradiation: the reaction was heated in the same reactor at 100 °C for 2 h (average power approximately 20 W). When performed in the planetary ball mills, the milling jar (50 mL, stainless steel) was charged with 48 milling balls (d = 5 mm) and 1500 milling balls (d = 2 mm). 10-undecynil-1-amine (0.275 g) and 1g of silica were added. Milling was accomplished at 200 rpm for 40 min. After cooling to room temperature, the modified silica was treated as previously described.

Preparation of Si-G-U-CD

Si-G-Und (1 g), 6-monoazido-β-CD (1.95 g, 1.68 mmol), $CuSO_4 \cdot 4H_2O$ (0.100 g, 0.4 mmol) and ascorbic acid (0.148 g, 0.84 mmol) were dissolved in H_2O (30 mL). The reaction was heated in the MW at 80 °C for 2 h (average power approximately 12 W). Silica was filtered, washed with water and dried under high vacuum. The silica was purified of the copper salts via the addition of Na_2H_2EDTA (3.14 g,), and dissolved in 5 mL H_2O. The suspension was left under magnetic stirring o.n.. The silica was then filtered, washed with water and dried under high vacuum.

Characterization of silica derivatives.

Thermogravimetric analyses were performed using a thermogravimetric analyzer TGA 4000 (Perkin Elmer) at 10 °C min^{-1} operating with alumina crucibles that contained 10-20 mg of

sample. The analyses were performed under O_2 atmosphere at a starting temperature of 45 °C and an end temperature of 800 °C. Total mass loss was attributed to the functional groups which were covalently attached to the sidewalls. UV-vis absorption spectra were measured on a dual-beam spectrophotometer (Agilent Technologies Cary 60,G6860AA) equipped with a 1 cm path length quartz cuvette. Elemental analyses were performed on an EA 1108 (Fison Instruments). Fourier transform infrared spectra (FTIR) were recorded on a Bruker IFS28 equipped with a MCT detector, working at a resolution of 4 cm^{-1} over 64 scans. Samples were in the form of self-supporting pellets which were suitable for infrared transmission experiments and were placed in a quartz cell equipped with KBr windows and designed for *in situ* activation and measurements. The samples were outgassed at room temperature before measurements to remove physically adsorbed water and impurities.

Specific surface area (SSA), pore volume and size were measured via nitrogen adsorption–desorption isotherms at -196 °C, using an ASAP 2020 gas-volumetric analyzer (Micromeritics). SSA was calculated using the Brunauer-Emmet-Teller (BET) method; average pore size and volume were calculated on the adsorption branch of the isotherms, according to the Barrett-Joyner-Halenda (BJH) method (Kruk-Jaroniec-Sayari equations). Prior to analyses, samples were outgassed at room temperature overnight.

High Resolution Transmission Electron Microscopy (HRTEM) observations were performed on a JEOL 3010 instrument operating at 300 kV. Powdered samples were dispersed on a copper grid coated with a perforated carbon film.

Sorption Experiments: Phenolphthalein

A buffer solution was prepared from 13.2 g Na_2CO_3 and 2.1 g $NaHCO_3$ dissolved in 250 mL of ultrapure water (pH = 10.5). Phenolphthalein (Php) powder was dissolved in ethanol to obtain

a 5 mM Php stock solution and β-CD powder was dissolved in ultrapure water to obtain a 0.88 mM β-CD stock solution. The Php stock solution was diluted in the buffer solution (pH = 10.5) to achieve a constant Php concentration of 0.008 mM and mixed with the β-CD stock solution to achieve β-CD concentrations of 0, 7.9, 9.6, 11.3, 13, 14.7, 16.4, 18.1 mmol l^{-1}. The absorbance of the CD calibration solutions was measured at a wavelength of 553 nm at room temperature. Si-G-U-CD samples (5 mg) were dispersed in a Php solution in buffer (0.008 mM, 5 mL). The mixture was stirred for 15 min at room temperature and filtered (0.45 μm cellulose acetate membrane filters, CPS Analitica, Italy). UV absorbance was recorded at 553 nm.

Sorption Experiments: Methyl Orange

An aliquot solution of methyl orange dissolved in water (2 mL), 0.5 mM, 1.5 mM, 2.5 mM, 4 mM, 6 mM, 10 mM) and silica based materials (10 mg) were added to a test tube and stirred for 2h. After the elimination of the solid via filtration, the UV absorbance of the solution was analyzed at 465 nm. Concentration was determined using a calibration curve and the equilibrium adsorption capacity was calculated. The Langmuir model was selected for the adsorption study. This model assumes monolayer adsorption onto the surface and that the distribution of the compound between the two phases is controlled by an equilibrium constant,[37] which can be expressed by the following equation:

$$Q_{ads} = \frac{\lambda \cdot Q_m \cdot [MO]_{eq}}{1 + \lambda \cdot [MO]_{eq}}$$

where Q_{ads} is the equilibrium constant, Q_m is the maximum adsorption capacity at the monolayer formation (mmol/g) and λ is the adsorption coefficient (l mmol^{-1}). Q_m and λ were calculated via the linearization of the Langmuir equation, as follows:

$$\frac{[MO]_{eq}}{Q_{ads}} = \frac{1}{\lambda \cdot Q_m} + \frac{[MO]_{eq}}{Q_m}$$

RESULTS AND DISCUSSION

Synthesis

The designed silica derivative consists of β-CD anchored to silica via an alkyl hydroxyl amino spacer (Scheme 1) and was prepared in three steps. In the first step, silica was derivatized with 3-glycidoxypropyltrimethoxysilane ($CH_2OCHCH_2O(CH_2)_3Si(OCH_3)_3$, GPMS). It was then reacted with 10-undecynil-1-amine (Und) to open the epoxide ring and finally, in the third step, a Cu-catalyzed azide-alkyne cycloaddition (CuAAC) with 6-monoazido-6-deoxy-β-CD gave the Si-G-Und CD derivative. The 10-undecynil-amine moiety is a spacer that allows the monomeric β-CD to retain its high accessibility (its preparation from 10-undecynil alcohol is described in the Supporting Information).[38] Silica's strong MW absorption prompted us to compare the chemical derivatization of silica under dielectric and conventional heating. The synthetic route was also studied using mechanochemical activation in solvent-free conditions.

Infrared spectra were acquired to identify the structure of the derivative obtained while thermogravimetry analyses were carried out to measure the loading obtained.
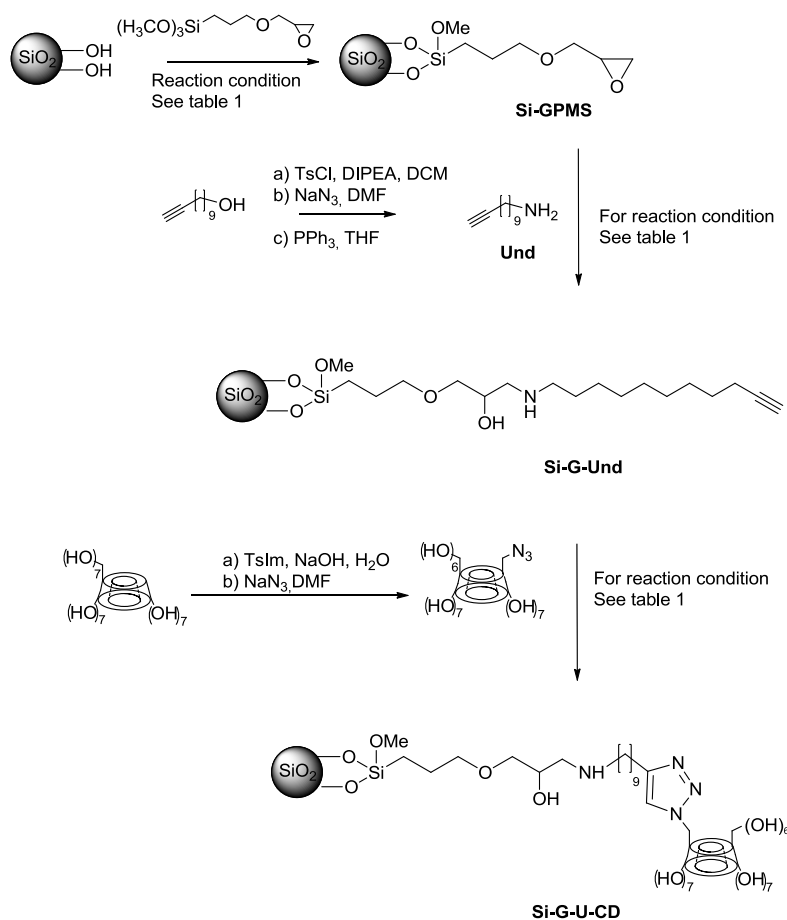
Table 1. Synthetic scheme for the preparation of Si-G-U-CD

As depicted in Table 1, the preparation of the Si-GPMS intermediate was performed under varying conditions. Because of significant interest in this versatile intermediate, which allows the post-grafting of the silica surface, emphasis was given to the optimization of Si-GPMS synthesis in the presence of (3-glycidoxypropyl)methyldiethoxysilane.[39-41] The experiments were performed both under conventional and dielectric heating with the aim of reducing reaction time and reagent amounts. The MW-assisted reaction in water was over in 1 h while conventional heating took 5 h.

A multimodal MW reactor operating at reduced pressure and equipped with a 45° tilted rotating reaction vessel was employed (Rotosynth, Milestone, Fig.1). The system was setup to

enable the gentle removal of solvents during the reaction. The reaction was performed with a reduced amount of GPMS (Entry 6, Table 1) at 80 °C until the powder was dry. In this case, the TGA analysis showed a lower degree of substitution when compared to the previous results. Highly efficient derivatization was obtained in solvent-free conditions in a planetary ball mill: In the presence of 300 µl/g silica of GPMS and after 20 minutes, the grafting efficiency measured by TGA was comparable to that obtained under MW irradiation with higher reagent amounts (Entry 7, Table 1). The Si-GPMS samples obtained from conventional and non-conventional procedures were subjected to the epoxide opening reaction with 10-undecynil-1-amine. On the basis of a preliminary optimization, using benzylamine as a model, DMF was selected as the best solvent and 1.64 mmol/g of amine was necessary to obtain satisfactory results (see Supporting Info). Despite poor results being obtained under conventional heating, MW irradiation was proven to increase reaction efficiency and cut reaction time (entry 9,10 Table 1). Remarkably high derivatization values were obtained in solvent-free conditions and under mechanochemical activation in 40 min.

It has been well established that the MW-promoted Cu-catalyzed 1,3-dipolar cycloaddition (CuAAC) between CD monoazides and monoacetylene moieties, which results in the formation of a triazole bridge, is the most efficient way to modify the CD surface.[42-44] Using this procedure, the Si-G-Und derivative was reacted with 6^I-deoxy-6^I-monoazido-β-CD. The reaction was successfully performed in water in the presence of $CuSO_4$ and ascorbic acid (entries 12-16). TGA analysis showed that the final loading was 135 µmol/g of β-CD when the three steps were all performed under MW irradiation and 92 µmol/g when steps 1 and 2 were carried out in solvent free conditions. When the synthetic scheme was performed in oil bath (entry 12) the final loading was 47 µmol/g

Table 1 Optimization of Si-G-U-CD preparation

Entry	Sample	Reaction condition[a]	Energy source[b] (step1,step2,step3)	Loading µmol/g[c]
1	Si-GPMS$_{ob}$	GPMS (934 µL/g silica), toluene, 80°C, 5h	Oil bath	364
2	Si-GPMS$_{ob}$	GPMS (934 µL/g silica), toluene, 80°C, 5 h	Oil bath	697
3	Si-GPMS$_{ob}$	GPMS (934 µL/g silica), H_2O, 80°C, 5h	Oil bath	698
4	Si-GPMS$_{MW}$	GPMS (934 µL/g silica), H_2O, 90°C, 1h	MW	665
5	Si-GPMS$_{MW}$	GPMS (934 µL/g silica), toluene, 100°C, 1h	MW	594
6	Si-GPMS$_{MW}$	GPMS (300 µL/g silica), H_2O, 80°C, 30 min	MW[d]	428
7	Si-GPMS$_{Me}$	GPMS (300 µL/g silica), 200 rpm, 20 min	Mecc	524
8	Si-G-Und$_{ob_{1,2}}$	Amine (1.64 mmol/g), DMF, 80°C, 24h	Oil bath$_1$, oil bath$_2$	101
9	Si-G-Und$_{MW_{1,2}}$	Amine (1.64 mmol/g), DMF, 100°C, 2h	MW$_1$, MW$_2$	352
10	Si-G-Und$_{Me_1,MW_2}$	Amine (1.64 mmol/g), DMF, 100°C, 2h	Mecc$_1$, MW$_2$	269
11	Si-G-Und$_{Me_{1,2}}$	Amine (1.64 mmol/g), 200 rpm, 40 min	Mecc$_1$, Mecc$_2$	209
12	Si-G-U-CD$_{ob_{1,2,3}}$	CuSO$_4$/Ascorbic Ac (0.4/0.8 mmol/g),	Oil bath$_1$, oil bath$_2$, Oil bath$_3$	47

		H$_2$O, 80°C, o.n.		
13	Si-G-U-CD$_{MW_{1,2,3}}$	CuSO$_4$/Ascorbic Ac (0.04/0.08 mmol/g) DMF/H$_2$O	MW$_1$, MW$_2$, MW$_3$	115
14	Si-G-U-CD$_{MW_{1,2,3}}$	CuSO$_4$/Ascorbic Ac (0.4/0.8 mmol/g), H$_2$O, 80°C, 2h	MW$_1$, MW$_2$, MW$_3$	135
15	Si-G-U-CD$_{Me_1,MW_{2,3}}$	CuSO$_4$/Ascorbic Ac (0.4/0.8 mmol/g), H$_2$O, 80°C, 2h	Mecc$_1$,MW$_2$,MW$_3$	68
16	Si-G-U-CD$_{Me_{1,2},MW_3}$	CuSO$_4$/Ascorbic Ac (0.4/0.8 mmol/g), H$_2$O, 80°C, 2h	Mecc$_1$,Mecc$_2$,MW$_3$	92

[a] the reaction conditions of the last step are described, [b] the energy source of each individual step, [c] loading was measured by TGA, [d] reaction performed in the MW-reactor Rotosynth , (Milestone, GmbH).

Figure 1. MW-reactor Rotosynth® (Milestone, GmbH).

Characterization

In Fig. 2 FTIR spectra of of silica gel, Si-GPMS, Si-G-Und and Si-G-U-CD are depicted. Only selected samples are showed because the FTIR analysis did not show significant differences between the various synthesis batches . The spectrum of the parent silica sample is also reported for comparison and is characterized by typical Si-OH stretching (ν) vibrations (3740 cm^{-1} assigned to the free silanols and broad absorption in the 3720-300 cm^{-1} range can be assigned to hydrogen bonded ones).[45-47] In the low frequency range, silica is characterized by a triplet of bands between 2100 and 1500 cm^{-1} which are caused by the overtones and combination modes of the intense SiO vibrations that fall below 1250 cm^{-1}.

The Si-GPMS derivative displayed weak but clear bands at 3020 and 2973 cm^{-1}, which are easily assigned to the νCH modes related to the epoxy ring (νC$_{epoxy}$–H), and are close to the typical alkyl chain (νC$_{alkyl}$–H) νCH$_2$ modes, at 2930 and 2870 cm^{-1}.[48] The corresponding bending modes (δCH$_2$ and δCH$_3$) are observed between 1500 and 1300 cm^{-1} and confirm the successful grafting of GPMS. This is further supported by a decrease in the Si-OH band at 3740 cm^{-1}. The typical epoxy ring breathing mode (expected between 1265 and 1245 cm^{-1}) is not visible as it is superimposed on the strong silica modes. We also noticed an increase in Si-OH hydrogen bonded group absorption (between 3700 and 300 cm^{-1}), which may be related to a hydrogen bonding interaction between the functional groups and the silica surface.

The bands ascribed to the epoxy ring disappear completely after reaction with 10-undecynil-1-amine (step 2 of Scheme 1) which is in accordance with the nucleophilic ring opening reaction (Si-G-Und). Another indication of the presence of an alkynyl moiety on silica is the appearance of bands at 3314-3310 cm^{-1} (νC$_{alkyne}$–H) and at 2116 cm^{-1} (νCalkyne–C). The occurrence of the

reaction is also displayed by the increase in the alkyl chain νCH_2 modes (now at 2930 and 2856 cm^{-1} with the corresponding δCH_2 in the low frequency region) and the intense νNH band at 1655 cm^{-1}. The hydrolysis of the unreacted methoxy group is shown by the disappearance of the νCH_3 and δCH_3 modes (νCH_3 at 2947 cm^{-1} and typical umbrella mode which was previously at 1340 cm^{-1}).

After the CuAAC reaction, the silica derivative (Si-G-U-CD) clearly displayed a lack of the signals for the alkynyl function and at 2116 cm^{-1}, while an intense, broad band appeared at 1628 (with a shoulder at 1584 cm^{-1}) and can be ascribed to triazolyl group ring vibrations. Moreover, the evident increase in absorption between 3720 and 2600 cm^{-1} (hydrogen bonded νOH, centered at 3376 cm^{-1}) and in the νCH_2 bands, together with the formation of intense bands at 1400 and 1364 cm^{-1} (δOH modes), confirm the presence of β-CD on the silica surface.
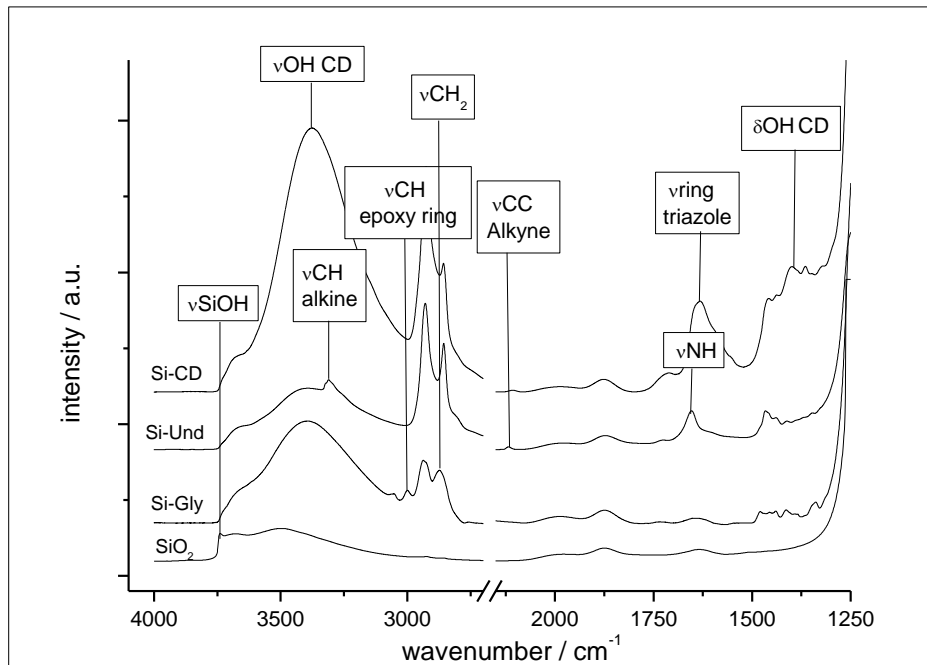

Figure 2. IR spectra of silica gel, Si-GPMS, Si-G-Und and Si-G-U-CD. Wavenumbers from 1250 to 4000 are shown.

Thermogravimetry analysis (TGA) allows the grafting efficacy of every single step to be quantified by assuming that water is the only compound removed from the starting silica by surface dehydroxylation. The TGA curves of the Silica, Si-GPMS, Si-G-Und and Si-G-U-CD samples obtained under MW promoted synthetic scheme (Entries 4, 9, 13, Table 1) are shown in Fig. 3. The curves are all normalized to 150°C to circumvent any possible solvent influence on yield calculations. The TGA curve of Si-GPMS shows that GPMS starts pyrolysis at 255 °C. When Si-G-U-CD was analyzed, we observed two degradation steps: the first starts at 305 °C while the second degradation step starts at 540 °C. TGA analyses proved that different conditions resulted in different grafting efficiencies and the results are listed in the Table 1 (more details are provided in the Supporting information).
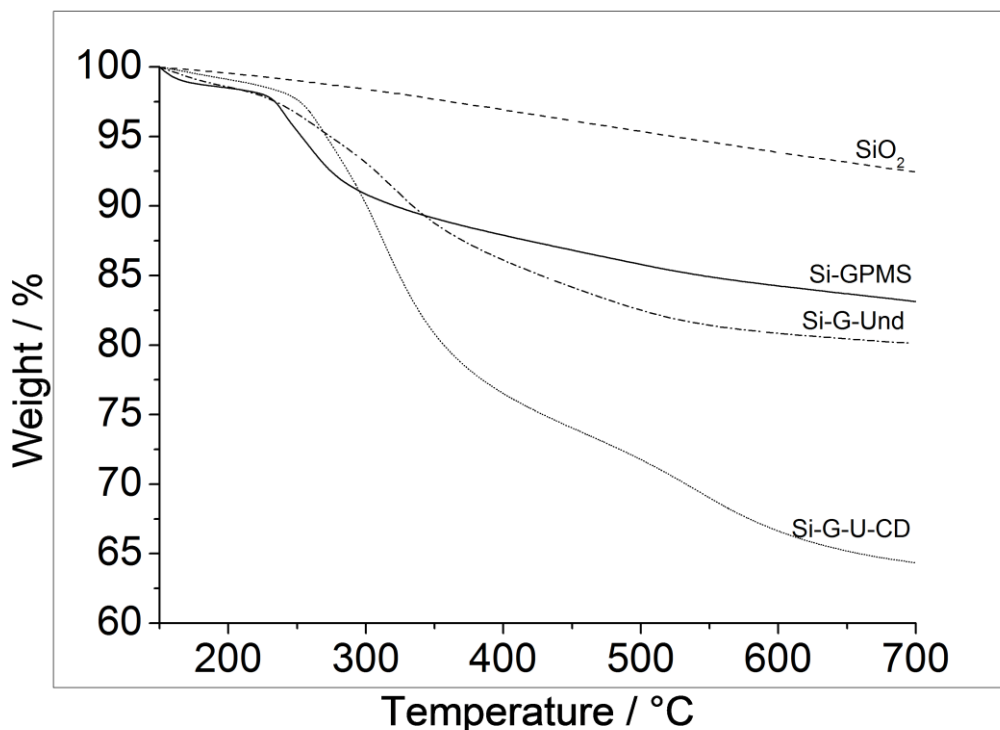

Figure 3. TGA profile of starting silica, Si-GPMS, Si-G-Und and Si-G-U-CD

Results of the elemental analyses are depicted in the Table 2. The sample obtained using the MW promoted protocol was analyzed to confirm the data obtained from TGA.

Table 2. Elemental analysis data

Sample [a]	% C	%H	%N	μmol/g (C)	μmol/g (N)
Si (SIPERMAT 320)	<0.1	0.7	<0.1	-	-
Si-GPMS$_{MW}$	5.8	2.14	<0.1	690	-
Si-G-Und$_{MW_{1,2}}$	10.58	2.35	0.9	361	448
Si-G-U-CD$_{MW_{1,2,3}}$	17.79	2.84	2.0	143	158

[a] Si-GPMS$_{MW}$ sample refers to the derivative depicted in Table 1, Entry 4; Si-G-Und$_{MW_{1,2}}$ sample refers to the derivative depicted in Table 1, Entry 9; Si-G-U-CD$_{MW_{1,2,3}}$ sample refers to the derivative depicted in Table 1, Entry 13;

The samples show significant increases in carbon content when comparing Si-GPMS to Si-G-Und and to Si-G-U-CD. (Table 2). Data are almost all in accordance with the TGA analysis, however, N% based Si-G-Und loading was overestimated because of the presence of DMF residues. The amounts of Und and β-CD can be calculated by subtracting the contribution of GPMS and GPMS-Und respectively.

Table 3. BET analysis data

Sample	Energy source (Step 1, step2, step3	SSA / m^2g^{-1}	Pore Volume / cm^3g^{-1}

SiO$_2$		173	0.95
Si-G-Und$_{MW_{1,2}}$	MW$_1$, MW$_2$	83	1.02
Si-G-U-CD$_{MW_{1,2,3}}$	MW$_1$, MW$_2$, MW$_3$	88	0.67
Si-G-U-CD$_{Me_1,MW_{2,3}}$	Mecc$_1$, MW$_2$, MW$_3$	38	0.28
Si-G-U-CD$_{Me_{1,2},MW_3}$	Mecc$_1$, Mecc$_2$, MW$_3$	67	0.32

[a] Si-G-Und$_{MW_{1,2}}$ sample refers to the derivative depicted in Table 1, Entry 9; Si-G-U-CD samples refer to the derivative depicted in Table 1, Entry 13-15;
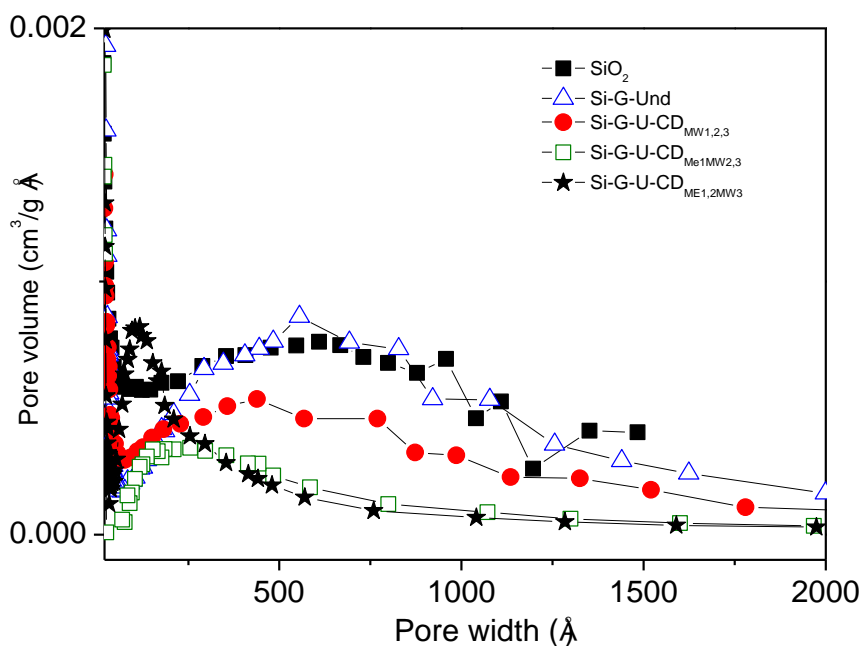

Figure 4. Pore size distribution of the samples listed in Table 3

The textural properties of the silica-based samples were characterized so as to obtain information on the changes induced by the various surface functionalization methods (MW and mechanochemistry). The main BET analysis results are summarized in Table 3 together with those from the parent silica sample for comparison. The samples display a type IV isotherm

17

which is typical of mesoporous materials. This reinforced by the relatively large SSA and pore volume of the samples. These features are the result of silica's small particle size (see below, HRTEM) which results in interparticle porosity. Sample pore size distributions, listed in Table 3, are reported in Fig. 4. The decrease in SSA as we pass from parent silica to Si-G-Und is in agreement with the covering of the surface with grafting chains. However, this does not affect the available pore volume, which is similar in the two samples, within experimental error. Pore size distribution (Fig. 4) is broad and centered around 500 nm in both samples. The only difference is found in a decrease in pore volume in the low size region (between 100 and 200 nm) of the Si-G-Und sample, which could be explained by the grafting groups occupying interparticle voids.

Both SSA and pore volume are affected, to varying degrees and according to preparation method, when β-CDs are covalently bonded to the linker. These values are apparently related and decrease, with respect to Si-G-Und, in the order $Si\text{-}G\text{-}U\text{-}CD_{MW_{1,2,3}} > Si\text{-}G\text{-}U\text{-}CD_{Me_1,MW_{2,3}} \equiv Si\text{-}G\text{-}U\text{-}CD_{Me_{12},MW_3}$. In the sample prepared in three MW steps, these changes are clearly related to a reduction in accessible volume caused by the presence of the relatively bulky β-CD. This does not greatly change the pore size distribution, however, as can be seen in Fig. 3, which is still roughly centered around 500 nm.

In the two samples prepared using one or two mechanochemical steps, the interpretation is less straightforward since changes in the textural properties may be due to the physical process itself (see also below, HRTEM results). Indeed, not only is pore volume relatively low in this case (0.28 and 0.32 with respect to 0.95 in the starting silica), but pore size distribution (Fig. 4) is shifted to lower values (maxima at 244 and 100 nm, respectively).

Sorption and inclusion capacity

18

The interaction between CD and Phenolphthalein (Php) was used to achieve the dual aims of investigating the inclusion capacity of grafted β-CD and discovering the amount of β-CD that maintains inclusive properties. [49-50] Php's distinctive purple color when above pH 8.4, is lost upon complexation with β-CD as its delocalization is disturbed by the lactonization of the ionized form (Scheme 2). [51-52] The characteristic Php peak around 550 nm decreases with additional amounts of β-CD and this absorbance change can be quantified by UV-vis spectroscopy.
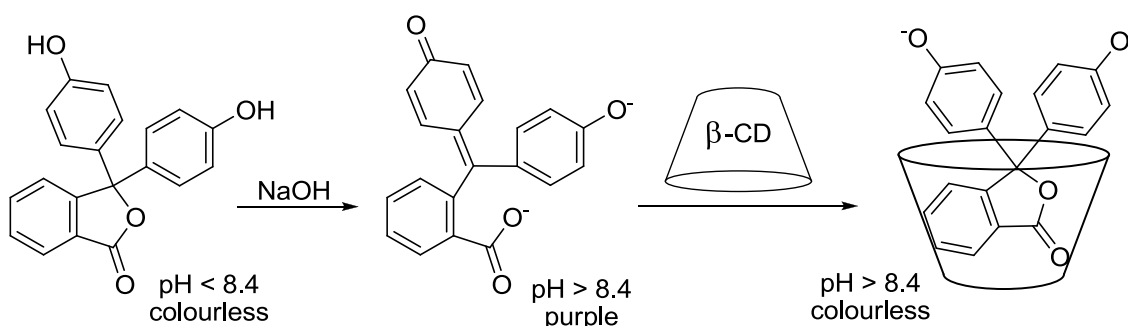
Scheme 2 Phenolphtalein/β-CD inclusion complex formation

If the formation of colourless Php : β-CD complex in alkaline aqueous solution has been used for the quantitative determination of β-CD content in the CD grafted silica derivative, the Methyl Orange (MO) was chosen as a probe molecule to evaluate the absorption properties capacity of this new material. [53,54] Furthermore MO gives stable inclusion complex with β-CD. [55]

Phenolphtalein

The UV profiles of Php solution treated with silica, Si-G-U-CD derivatives demonstrate that the Php is selectively included by β-CD and any decrease in UV adsorbance wasn't observed with silica and the silica intemediates Si-GPMS, Si-G-Und (Fig.5). For this reason we decided to employ Php to quantify the CD present on the surface of silica that is able to include organic molecules. The procedure is rapid and easy; powders are dispersed into a Php solution, and the

change in Php absorbance is recorded on a UV spectrophotometer. It was observed that Php

solution absorbance decreased significantly in the presence of derivatized silica and that the

change in absorbance was close to complete in 10 min. After the analysis of the three Si-G-U-

CD samples, the amount of CD which was free and able to include Php was measured via

comparison with the calibration curve (see Table 3). We observed that the inclusion capacity of

the grafted β-CD was mainly maintained in relation to TGA data. The samples prepared in one or

two steps under mechanochemical activation showed only slightly reduced complexation

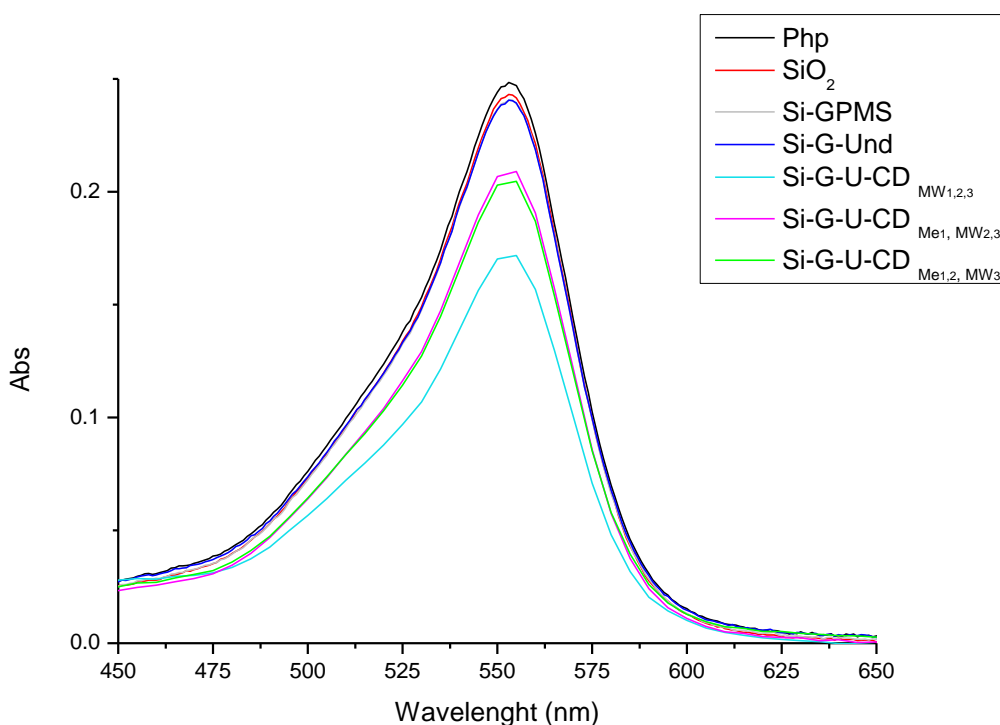properties, although the BET analysis did show some changes in textural properties.

Figure 5. UV-Vis spectra of Php, in presence of SiO_2, Si-GPMS, Si-G-Und and Si-G-U-CD. The presence of colorless Php:βCD inclusion complex is evidenced by the decrease in absorbance of Php solution.

Table 3 Phenolphthalein titration data

Sample	Energy source (Step 1, step2, step3)[a]	β-CD (μmol/g)
Si-G-U-CD$_{MW_{1,2,3}}$	MW$_1$, MW$_2$, MW$_3$	96
Si-G-U-CD$_{Me_1,MW_{2,3}}$	Mecc$_1$, MW$_2$, MW$_3$	64
Si-G-U-CD$_{Me_{1,2},MW_3}$	Mecc$_1$, Mecc$_2$, MW$_3$	68

[a] the reaction conditions are depicted in Table 1 Entry 13-15

Sorption capacity

The capacities of Silica, Si-G-Und $_{MW_{1,2}}$ (entry 9 Table 1) and Si-G-U-CD $_{MW_{1,2,3}}$ to adsorb methyl orange (Tab. 1, Entry 13) were studied at room temperature, as and additional information about the surface properties of the materials. The resulting data are reported in Fig. 6. Methyl orange clearly displays low affinity towards bare silica, giving a very small adsorption in the whole range of concentrations employed in this study. On the contrary the adsorbed amount drastically increases on Si-G-Und $_{MW_{1,2}}$ and further more on Si-G-U-CD $_{MW_{1,2,3}}$(123 mmol/g for and 200 mmol/g, respectively at the highest concentration employed in this study). This evident increase in the adsorption capacity can be thus ascribed to methyl orange interactions with the surface functional groups and βCD, respectively.

Freundlich and Langmuir adsorption isotherms were used to model the equilibrium adsorption data of Si-G-Und$_{MW_{1,2}}$ and Si-G-U-CD$_{MW_{1,2,3}}$ samples, by employing the corresponding linear equations. This was not performed on the SiO$_2$ data due to low adsorption capacity. The adsorption data fitted relatively well with both models, but gave a better fit to the Langmuir model (Fig. 7), as evidenced from the higher value of R^2 correlation coefficient (Table 4). For

sake of brevity the results obtained with the Freundlich model are reported in the Supplementary Information (Figure S7 and Table S1).

The Langmuir model was also preferred since it is based on a physical model, at variance with the empirical nature of Feundlich equation. This allows the calculation of Q_m, the monolayer capacity of the substrate and of λ, which can be assimilated to the thermodynamic equilibrium constant of the adsorption process. The latter is thus related to the heat of adsorption, in turn giving information on the affinity between adsorbent and substrate. The resulting values are summarized in Table 4, where the Q_m value for silica (reported for comparison) was estimated from the adsorption data. The corresponding values for Si-G-Und to Si-G-U-CD are reasonable and demonstrate that the Si-G-Und intermediate derivative showed good sorption capacity which is due to the co-presence of hydrophilic functions, such as amino and hydroxyl groups, and a hydrophobic chain. The presence of the CD provides further improvement and a small decrease in the λ value. The same trend was observed with the Freundlich model (Supplementary Information).

Finally, we believe that the good Langmuir model fitting of experimental data we achieved, assuming homogeneous adsorption sites and the formation of a monolayer, is proof of the specificity of the methyl orange interaction with the surface. In other words, this confirms the presence of the structures proposed in Scheme 1 and the availability of β-CDs as adsorption sites.
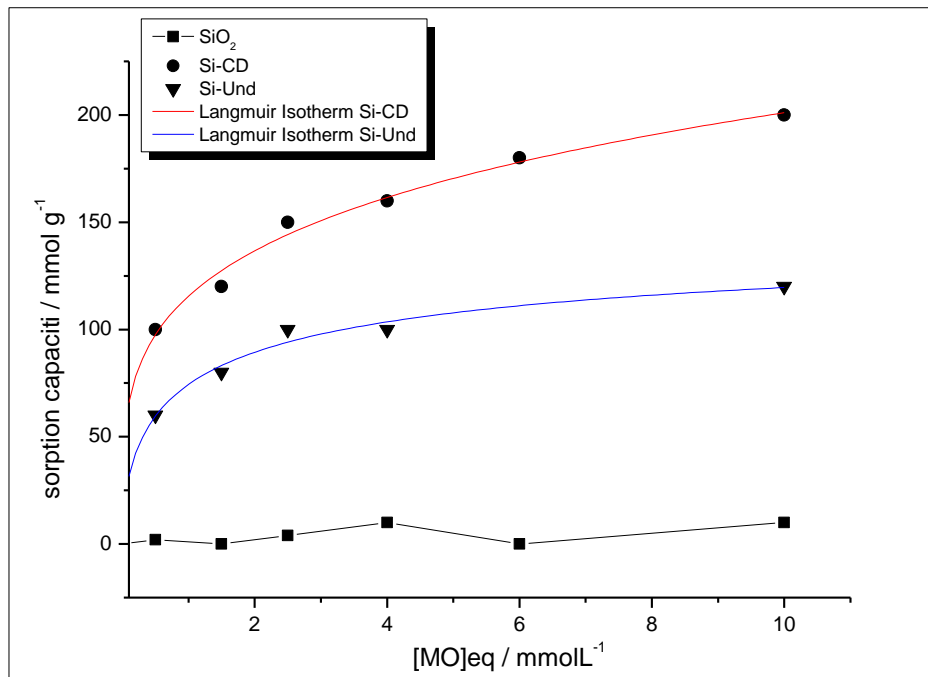
Figure 6. Adsorption isotherm of MO with SiO2 (Black), Si-G-U$_{MW_{1,2}}$ (blue) and Si-G-U-CD$_{MW_{1,2,3}}$ (red).
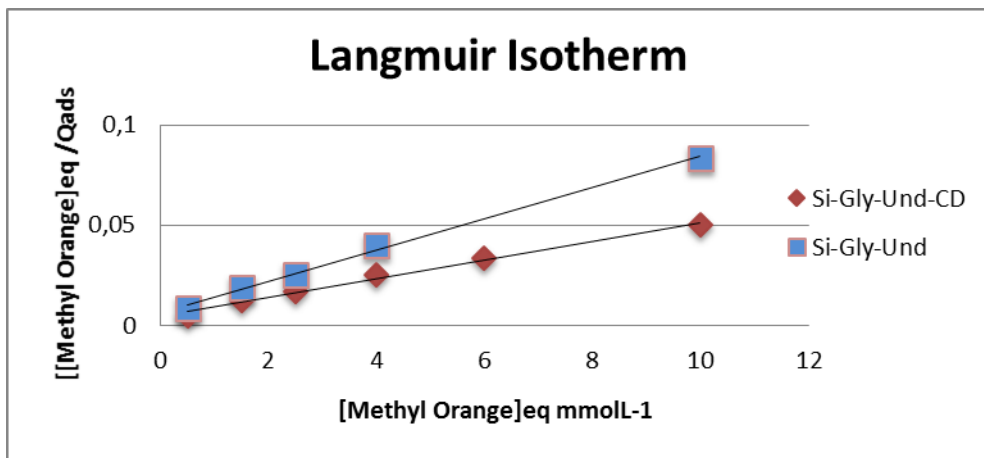

Figure 7. Langmuir isotherm Si-G-U$_{MW_{1,2}}$ (◊) and Si-G-U-CD$_{MW_{1,2,3}}$ (□).

Table 4 Langmuir constants for adsorption process

Sample	Langmuir treatment

	$1/Q_{ads}=(1/\lambda \cdot Q_m)*(1/[Mo]_{eq})+1/Q_m$	
SiO$_2$	Qm= 11.0*	mmol/g
	λ= not available	l mmol^{-1}
Si-G-U$_{MW_{1,2}}$	Qm=128.2	mmol/g
	λ=1.258	l mmol-1
	R^2=0.9966	
Si-G-U-CD$_{MW_{1,2,3}}$	Qm=217.4	mmol/g
	λ=0.958	l mmol-1
	R^2=0.9926	

* Q$_m$ not calculated with Langmuir model but estimated from adsorption plot

High Resolution Transmission Electron Microsocopy (HRTEM)

HRTEM was used to study the morphology of the silica-based samples and particular attention was paid to the changes induced by the functionalization methods. The parent silica material is formed of small and irregular spherical particles (around 10 nm in size) which form large aggregates (Fig. 8). The presence of interparticle voids, which result in high SSA and pore volume, can be appreciated in this image. This picture is quite similar to what was observed in the Si-G-U-CD$_{MW_{1,2,3}}$ sample (panel b) and is in agreement with gas-volumetric analysis observations (see above).

It is safe to deduce that the morphology of the sample was not dramatically changed by mechanochemical treatment as large agglomerates of small particles can be still observed in the HRTEM analysis (panels c and d). However, the agglomerates appear to be denser in both cases, suggesting that the physical process could have caused a partial sintering of the silica nanoparticles. This may thus explain the larger decrease in SSA and pore volume found in these sample over the MW only sample (Si-G-U-CD$_{MW_{1,2,\textbf{3}}}$).
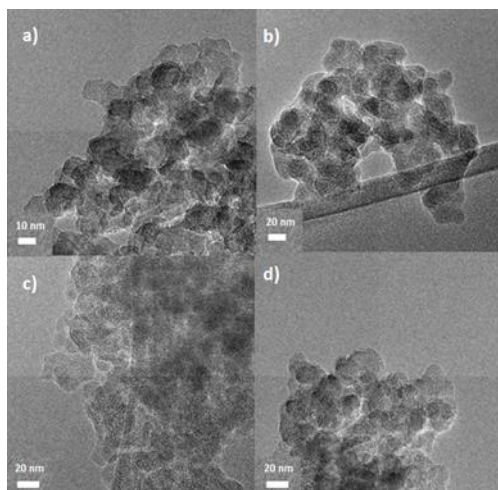
Figure 8. HRTEM images of a) SiO_2 (150000 X); b) Si-G-U-$CD_{MW_{1,2,3}}$ (80000 X); c) Si-G-U-$CD_{Me_1MW_{2,3}}$ (100000 X) d) Si-G-U-$CD_{Me_{1,2}MW_3}$ (100000 X)

CONCLUSION

In conclusion, β-CD was efficiently grafted onto the surface of silica particles by means of sustainable protocols using non-conventional methods. The study has demonstrated that MW irradiation can promote all the steps in the synthetic route and that three time higher loading values can be obtained when compared to the silica derivatized in oil bath (135 µmol/g *vs* 47 µmol/g). Green, solvent-free mechanochemical activation leads to an outstanding grafting process. Exhaustive characterization of the final derivatives has demonstrated that the inclusive capabilities of β-CD were maintained in all the samples. The high efficiency of these grafting procedures paves the way for novel applications for this versatile system.

ACKNOWLEDGMENTS

SUPPORTING INFORMATION.

This information is available free of charge via the Internet at http://pubs.acs.org/.

REFERENCES

(1) Fihri, A.; Bouhrara, M.; Nekoueishahraki, B.; Basset, J.-M.; Polshettiwar, V. Nanocatalysts for Suzuki cross-coupling reactions. *Chem. Soc. Rev.* **2011**, *40*, 5181–5203.

(2) Asefa, T.; Tao, Z. Mesoporous silica and organosilica materials - Review of their synthesis and organic functionalization. *CJC.* **2012**, *90*, 1015-1031.

(3) Slowing, I.; Vivero-Escoto, J.L.; Trewyn, B.G.; Lin, V.S.-Y. Mesoporous silica nanoparticles: structural design and applications. *J. Mater. Chem*. **2010,** *20*, 7924–7937.

(4) Dacquin, J.-P.; Cross, H. E.; Brown, D. R.; Duren, T.; Williams, J. J.; Lee, A. F.; Wilson, K. Interdependent Lateral Interactions, Hydrophobicity and Acid Strength and Their Influence on the Catalytic Activity of Nanoporous Sulfonic Acid Silicas. *Green Chem.* **2010**, *12*, 1383-139.

(5) G. Berlier,; L.Gastaldi, E. Ugazio, I. Miletto, P. Iliade, S. Sapino, J. Stabilization of quercetin flavonoid in MCM-41 mesoporous silica: positive effect of surface functionalization, *Colloid Interf. Sci*. **2013**, *393*, 109–118.

(6) Park, J.W.; Park Y.J.; and Jun C.-H. Post-grafting of silica surfaces with pre-functionalized organosilanes: new synthetic equivalents of conventional trialkoxysilanes. *Chem. Commun.* **2011**, *47*, 4860–4871.

(7) Jonkheijm, P.; Weinrich, D.; Schröder, H.;. Niemeyer, C. M; Waldmann, H. Chemical Strategies for Generating Protein Biochips. *Angew. Chem. Int. Ed*. **2008**, *47*, 9618-9647.

(8) Hudson, S.; Cooney, J.; Magner, E. Proteins in Mesoporous Silicates. *Angew. Chem. Int. Ed.* **2008**, *47,* 8582-8594.

(9)   P. Jonkheijm, D. Weinrich, H. Schröder, C. M. Niemeyer and H. Waldmann, Chemical Strategies for Generating Protein Biochips. *Angew. Chem., Int. Ed.,* **2008**, *47*, 9618.

(10)   Yiu, H. H. P.; Wright, P. A.; Enzymes supported on ordered mesoporous solids: a special case of an inorganic–organic hybrid. *J. Mater. Chem.* **2005**, *15*, 3690-3700.

(11)   Barge, A.; Tagliapietra, S.; Binello, A.; Cravotto, G. Click Chemistry Under Microwave or Ultrasound Irradiation. *Curr. Org. Chem.* **2011**, *15*, 189-203.

(12)   Guerrouache, M.; Millot, M.-C.; Carbonnier B. Functionalization of Macroporous Organic Polymer Monolith Based on Succinimide Ester Reactivity for Chiral Capillary Chromatography: A Cyclodextrin Click Approach *Macromol. Rapid Commun.* **2009**, *30*, 109–113.

(13)   Wang, H.; Peng, J.; Wei, J.; Jiang A. Synthesis of Novel Chiral Stationary Phase Based on Atom Transfer Radical Polymerization and Click Chemistry *Acta Chimica Sinica* **2012**, *70*, 1355-1361.

(14)   Varma, R.S. Journey on greener pathways: from the use of alternate energy inputs and benign reaction media to sustainable applications of nano-catalysts in synthesis and environmental remediation. *Green Chem.* **2014**, *16*, 2027-2041.

(15)   Schröder, K.; Matyjaszewski, K.; Noonan, K. J. T.; Mathers, R. T. Towards sustainable polymer chemistry with homogeneous metal-based catalysts. *Green Chem.* **2014**, *16*, 1673-1686.

(16)   Dallinger, D.; Kappe, C. O. Microwave-Assisted Synthesis in Water as Solvent. *Chem. Rev.* **2007**, *107*, 2563−2591.

(17) Chanda, A.; Fokin, V.V. Organic Synthesis "On Water". *Chem. Rev*. **2009**, *109*, 725–748.

(18) Cave, G. W. V.; Raston, C. L.; Scotta, J. L. Recent advances in solventless organic reactions: towards benign synthesis with remarkable versatility. *Chem. Commun*. **2001**, 2159–2169.

(19) Polshettiwar, V.; Varma, R. S. Microwave-Assisted Organic Synthesis and Transformations using Benign Reaction Media. *Acc. Chem. Res.* **2008**, *41*, 629-639.

(20) Cravotto, G.; Orio, L.; Gaudino, E.C.; Martina, K.; Tavor, D.; Wolfson, A.; New efficient synthetic protocols in glycerol under heterogeneous catalysis. *ChemSusChem*. **2011,** *4*, 1130-1134.

(21) Gaudino, E. C.; Carnaroglio, D.; Nunes, M. A. G.; Schmidt, L.; Flores, E. M. M.; Deiana, C.; Sakhno, Y.; Martra, G.; Cravotto, G. Fast TiO_2-catalyzed direct amidation of neat carboxylic acids under mild dielectric heating. *Catal. Sci. Technol*. **2014**, *4*, 1395–1399.

(22) Stolle, A.; Szuppa, T.; Leonhardt, S. E. S.; Ondruschka, B. Ball milling in organic synthesis: solutions and challenges. *Chem. Soc. Rev.* **2011**, *40*, 2317–2329.

(23) Schurig, V.; Wistuba, D. Recent innovations in enantiomer separation by electrochromatography utilizing modified cyclodextrins as stationary phases. *Eletcrophoresis*. **1999**, *20*, 2313-2328.

(24) Dai, Y.; Tang, W.; Wang, Y.; Ng. S-C. Chromatographic Separations and Analysis: New Stationary Phases. *Comprehensive Chirality*. **2012**, *8*, 286-310.

(25) Janus, L.; Carbonnier, B.; Deratani, A.; Bacquet, M.; Crini, G.; Laureyns J.; Morcellet, M.; New HPLC stationary phases based on (methacryloyloxypropyl β-cyclodextrin-co-N-vinylpyrrolidone) copolymers coated on silica. Preparation and characterisation *New J. Chem.,* **2003**, *27*, 307–312.

(26) Frost, C. G.; Mutton, L. Heterogeneous catalytic synthesis using microreactor technology. *Green Chem*. **2010**, *12,* 1687–1703.

(27) Minsker, L.; Renken, A. Pd/SiO2 catalysts: synthesis of Pd nanoparticles with the controlled size in mesoporous silicas. *J. Mol. Catal. A: Chem.* **2003,** *192*, 239–251.

(28) Calo, V.; Nacci, A.; Monopoli, A.; Fornaro, A.; Sabbatini, L.; Cioffi, N.; Ditaranto, N. Heck Reaction Catalyzed by Nanosized Palladium on Chitosan in Ionic Liquids *Organometallics.* **2004**, *23*, 5154-5158.

(29) Corma, A. From Microporous to Mesoporous Molecular Sieve Materials and Their Use in Catalysis *Chem. Rev.* **1997**, *97*, 237-2419.

(30) Khalafi-Nezhad, A.; Panahi, F. Size-Controlled Synthesis of Palladium Nanoparticles on a Silica−Cyclodextrin Substrate: A Novel Palladium Catalyst System for the Heck Reaction in Water *ACS Sustainable Chem. Eng..* **2014**, *2*, 1177-1186.

(31) Park, C.; Kim, H.; Kim, S.; Kim, C. Enzyme Responsive Nanocontainers with Cyclodextrin Gatekeepers and Synergistic Effects in Release of Guests *J. Am. Chem. Soc.* **2009,** *131*, 16614–16615.

(32) Yang, Y.-W. Towards biocompatible nanovalves based on mesoporous silica nanoparticles. *Med. Chem. Commun.* **2011**, *2*, 1033-1049.

(33) Yang, Y.-W.; Sun, Y.-L; Song, N. Switchable Host–Guest Systems on Surfaces. *Acc. Chem. Res*. **2014**, *47*, 1950-1960.

(34) Ferris, D. P.; Zhao Y.-L.; Khashab N. M.; Khatib H. A; Stoddart J. F. Light-operated mechanized nanoparticles. *J. Am. Chem. Soc.* **2009**, *131*, 1686-1688.

(35) A) Ponchel, A.; Abramson, S.; Quartararo, J.; Bormann, D.; Barbaux, Y.; Monflier, E. Cyclodextrin silica-based materials: advanced characterizations and study of their complexing behavior by diffuse reflectance UV–Vis spectroscopy. *Microporous and Mesoporous Materials.* **2004**, *75*, 261-272.

(36) Nielsen, R.; Kingshott, P.; Uyar, T.;. Hacalogluc, J.; Larsen, K. L. Characterization of β-cyclodextrin modified SiO_2. *Surf. Interface Anal.* **2011,** *43*, 884–892.

(37) Mazzotti M. Equilibrium theory based design of simulated moving bed processes for a generalized Langmuir isotherm. *J Chromatogr A*. **2006,** *1126*, 311–322.

(38) Barge, A.; Caporaso, M.; Cravotto, G.; Martina, K.; Tosco, P.; Aime, S.; Carrera, C.; Gianolio, E.; Pariani, G.; Corpillo, D. *Chem. Eur. J.* **2013,** *19*, 12086-12092.

(39) Yang, L.; Gao, Z., Guo, Y., Zhan, W.; Guo, Y.; Wang, Y., Lu G. Paramagnetic epoxy-functionalized mesostructured cellular foams with an open pore system for immobilization of penicillin G acylase. *Microporous Mesoporous Mater.* **2014,** *190*, 17–25.

(40) Feng, M.; Zhan, H. Facile preparation of transparent and dense CdS–silica gel glass nanocomposites for optical limiting applications. *Nanoscale* **2014**, *6*, 3972–3977

(41) Kudina, O.; Zakharchenko, A.; Trotsenko, O.; Tokarev, A.; Ionov, L.; Stoychev, G.; Puretskiy, N.; Pryor, S.W.; Voronov, A.; Minko, S. Highly Efficient Phase Boundary Biocatalysis with Enzymogel Nanoparticles. *Angew. Chem. Int. Ed*. **2014**, *53*, 483-487.

(42) Cintas, P.; Martina, K.; Robaldo, B.; Garella, D.; Boffa, L.; Cravotto, G. Improved protocols for microwave-assisted Cu(I)-catalyzed Huisgen 1,3-dipolar cycloadditions. *Collect. Czech. Chem. Commun*. **2007**, *72*, 1014–1024.

(43) Cintas, P.; Barge, A.; Tagliapietra, S.; Boffa, L.; Cravotto G. Alkyne–azide click reaction catalyzed by metallic copper under ultrasound. *Nat. Protoc*. **2010**, *5*, 607-616.

(44) Wang, Y.; Young, D.J.; Tana, T.T.Y.*;* Ng, S. "Click" preparation of hindered cyclodextrin chiral stationary phases and their efficient resolution in high performance liquid chromatography. *J. Chromatogr. A.* **2010**, *1217*, 7878–7883.

(45) Cauvel, A.; Brunel, D.; DiRenzo, F.; Garrone, E.; Fubini, B. Hydrophobic and Hydrophilic Behavior of Micelle-Templated Mesoporous Silica. *Langmuir*. **1997,** *13*, 2773-2778.

(46) Sacchetto, V.; Gatti G.; Paul G.; Braschi, I.; Berlier G.; Cossi, M.; Marchese, L.; Bagatin R.; Marchese L. "The interactions of methyl tert-butyl ether on high silica zeolites: a combined experimental and computational study" *Phys. Chem. Chem. Phys*., **2013**, *15*, 13275-13287.

(47) Balantseva, E.; Miletto I., Coluccia, S.; Berlier, G. "Immobilisation of Zinc porphyrins on mesoporous SBA-15: Effect of bulky substituents on the surface interaction, *Microporous Mesoporous Mater.* **2014**, *193,* 103–110.

(48) Socrates, G., Infrared and Raman Characteristic Group Frequencies; Third ed.; John Wiley & Sons Ltd: Chichester, England, **2006**.

(49) Mohamed, M. H.; Wilson, L. D.; Headley, J. V. Estimation of the surface accessible inclusion sites of β-cyclodextrin based copolymer materials. *Carbohydr. Polym*. **2010**, *80*,186–196.

(50) Zhao, Y.X.; Ding, M.Y.; Chen D.P. Adsorption properties of mesoporous silicas for organic pollutants in water *Anal. Chim. Acta* **2005**, *542*, 193–198.

(51) Anbia, M. Hariri, S.A.; Ashrafizadeh, S.N. Adsorptive removal of anionic dyes by modified nanoporous silica SBA-3 *Appl. Surf. Sci*. **2010**, *256*, 3228–3233

(52) Carrazana, J.; Reija, B.; Ramos Cabrer, P.; Al-Soufi, W.; Novo, M.; Tato J.V. Complexation of Methyl Orange with b-cyclodextrin: Detailed Analysis and Application to Quantification of Polymer-bound Cyclodextrin *Supramol. Chem.,* **2004**, *16* , 549–559

(53) Uyar, T.; Havelund, R.; Hacaloglu, J.; Besenbacher, F.; Kingshott, P. *ACS Nano*. **2010**, *4*, 5121-5130.

(54) Taguchi K. Transient Binding Mode of Phenolphthalein-β-Cyclodextrin Complex: An Example of Induced Geometrical Distortion. *J Am Chem Soc*. **1986**, *108*, 2705-2709.

(55) Buvári, A.; Barcza, L. Complex Formation of Phenolphthalein and Some Related Compounds with β-Cyclodextrin. *J. Chem. Soc. Perkin Trans* **1988**, *2*, 1687–1690.

For Table of Contents Use only

Efficient green protocols for the preparation of highly functionalized β-cyclodextrin grafted silica

Katia Martina†, Francesca Baricco†, Gloria Berlier‡, Marina Caporaso†and Giancarlo Cravotto,†*
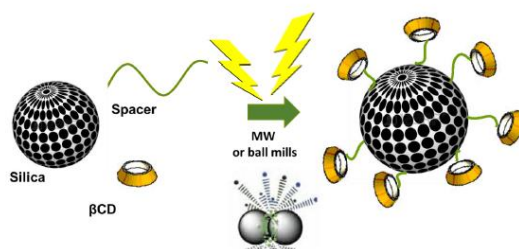
A non conventional approach for the synthesis of β-cyclodextrin grafted silica; microwave irradiation, benign reaction media and a solvent-free planetary ball mill have been applied to obtain an high degree of functionalization.